Science Arts & Métiers (SAM)

is an open access repository that collects the work of Arts et Métiers Institute of Technology researchers and makes it freely available over the web where possible.

This is an author-deposited version published in: https://sam.ensam.eu
Handle ID: .http://hdl.handle.net/10985/18544

To cite this version :

Nicolas CONIGLIO, N. SPITZ, M. EL MANSORI - Designing metallic surfaces in contact with hardening fresh concrete: A review - Construction and Building Materials - Vol. 255, p.119384 - 2020

Any correspondence concerning this service should be sent to the repository Administrator : scienceouverte@ensam.eu

Arts et Métiers Institute of Technology

Designing Metallic Surfaces in Contact with Hardening Fresh Concrete: a Review

N. Coniglio [a,*], N. Spitz [a], M. El Mansori [a,b]

[a] *Arts et Métiers ParisTech, MSMP-EA7350 Laboratory, Cours des Arts et Métiers, 13617 Aix-en-Provence, France*

[b] *Texas A&M Engineering Experiment Station, College Station, TX 77843, USA*

[*] corresponding author : nicolas.coniglio@ensam.eu

I. Abstract

Concrete, a commonly used material in the construction industry, interacts with metallic surfaces such as formwork during pouring and reinforced bar during lifespan. Formworks are designed to minimize hardened concrete adherence in order to avoid wall defects after formwork removal. In opposite, reinforced bar designs aim at maximizing their adherence to concrete for optimizing the transmission of mechanical solicitations. The present review investigates the surface properties that govern bonding of freshly poured concrete onto metallic surfaces. Identifying the underlying mechanisms of adhesion highlighted the importance of substrate characteristics (roughness, composition), concrete curing and compaction), and interfacial additives (release agents, wetting). This paper addresses the basic requirements in designing a functional surface interacting with concrete and emphasizes today challenges.

Keywords: *Concrete, Adherence, Adhesion, Metallic Substrate*

II. Introduction

Concrete is a mixture of hydrated cement paste and selected aggregates enabling the manufacturing of strong, durable and economical structures. In the construction industry, reinforced concrete walls are mostly built by using reinforced metallic prebars to improve mechanical properties and formworks to maintain the concrete during curing. Both concrete and interacting metallic surfaces must be correctly designed for reliable constructions.

Controlling the flow of fresh concrete is complex due to its small workability [1,2] which can be improved with the addition of superplasticizers. The cement paste is an alkaline calcium-containing solution composed of cement, filler, sand, gravel, and water. The residual water left after cement hydration contains soluble ions such as Ca^{2+}, OH^-, Na^+, K^+, and SO_4^{2-} [3]. The alkaline cations (Na^+ and K^+) and anions (OH^-) present in the liquid concrete phase leads to a very high pH (from 12 to 14 pH) that depends on the nature of the cement and its degree of hydration [3]. The chemical specificities of the concrete involve unique interfacial phenomena when interacting with metals.

Formworks are rigid molds used to contain freshly poured concrete for wall construction. Even though some composite slabs are used as permanent structures [4], most of them are removed after concrete curing to reveal the inherent aesthetic of the concrete wall [5–10]. Metal, wood, and polymer are used as formwork materials depending of the expected lifespan, geometry of the wall, and the weather during the construction day [7,11]. Avoid aesthetic defects related to formwork removal involve lowering concrete adherence which implies the application of release agents [12–22], the addition of a polymer skin [7,23], or some specific procedures for the formwork removal [6,24]. But these are challenging requirements because excessive sticking of concrete on formwork still induces today constructive anomalies for almost 80% of the constructed walls [25,26].

Reinforced bars are designed to maximize the bond strength between the bar and the hardened concrete [27]. The design is therefore similar to concrete repairs systems [28–31]. Adequate designs favor mechanical anchoring and physicochemical interactions at the interface between the concrete and the bar [12,24,32–34]. Moreover to the design of the bar itself, the orientation of the reinforced bar in regards to the gravity is important as the Interfacial Transition Zone (ITZ) is different at the lower and upper sides of horizontal reinforced bars [35]. Thus, both superficial characteristics and orientation of reinforced bars must be accounted for.

Concrete interaction with both formworks and reinforced bars start as soon as the fresh concrete contacts the metallic substrate. Identifying the underlying mechanisms creating adhesion and adherence during the curing process will help in designing proper surfaces. Adhesion refers to the physico-chemical phenomena that create a resistance when separating two surfaces. Adherence relates to the static friction that hinders the relative motion of two surfaces. The present review aims at providing a perspective on evaluating the interfacial behaviors and designing solid surfaces. As it is beyond the scope of this article to address cement and concrete formulations, only the interfacial mechanisms and the implications on the design will be reviewed. This review is presented in three sections: concrete-metal interaction phenomena, interfacial transition zone characteristics, and trends for future investigations.

III. Concrete-Metal interaction phenomena

Concrete is a strong alkaline medium composed of an hydrated mixture of cement and aggregate with some residual water containing soluble components (Ca^{2+}, OH^{-}, Na^{+}, K^{+}, and SO_4^{2-}) and fine particles of cement and filler [3]. The residual water displaces towards the metallic surface (referred to as wall effect) to form a boundary layer named the Interfacial Transition Zone (ITZ). Once cured, the ITZ is rich in weak hydrated phases (i.e., calcium hydroxide $Ca(OH)_2$) and may possibly exhibit porosities for high water-to-cement ratios [10,36]. A knowledge of the physics behind the interaction of concretes with metals is key for designing surfaces with desired interaction behaviors.

Adhesion of concrete to metal is developing progressively during concrete curing along the ITZ [37]. The ITZ is organized in three superimposed layers [36,38,39] that result from various simultaneous phenomena such as sedimentation, segregation, water permeation, wall effect, and mechanical vibrations. The first 10^1-10^2 µm-thick layer along the substrate is composed of the finest cement particles and water with additions of cement substituents and admixtures. The intermediary 5 mm-thick layer is the mortar layer containing large sand grains, cement, and water. The last layer is the concrete bulk itself with the biggest granulates which have a size of approximately 30 mm.

Mechanical anchoring through concrete penetration into the surface asperities and trapping of cement particles in hollows [12,17,24,32], capillary suction induced by a continuous water film formed on planar surfaces [12,17,32,33], and electrochemical bonding with $Ca(OH)_2$ formation [24,33,34] are underlying mechanisms of concrete adhesion. If the ITZ strength exceeds the concrete bulk strength, the rupture will be cohesive in the concrete bulk. However, a weaker ITZ promotes adhesive rupture along the substrate-concrete interface, i.e. the ITZ.

A. Mechanical Anchoring

The mechanical anchoring theory states that bonding forms by mechanical interlocks when the fines of the fresh concrete penetrate into substrate irregularities prior to curing. The adhering efficiency depends on the amount of potentially bonded areas that is controlled by the substrate surface texture itself. A correctly designed adherent texture for reinforced bars must favor penetration of concrete in surface defects [40]. In particular, the Wenzel wetting mode is preferred to a Cassie-Baxter regime to facilitate the penetration of the fines into the rough asperities [24,41,42]. The addition of superplasticizer in the concrete formulation has, in this regard, a positive effect by improving the wetting of the substrate and reducing the defects along the ITZ.

High substrate roughness such as the use of ribbed bars, higher hydrophilicity, high pressures at the wall bottoms (from 1 to 10 $t.m^{-2}$) [43–45] and mechanical vibrations sustaining filling of interspaces by fresh concrete [24,27,46,47] are main factors that improve the bonding. Mechanical anchoring is raised by eliminating any residual humidity film on the substrate before the concrete contacts the substrate [12,17,32] combined with a substrate roughness high enough to entrap more than one single particle per asperity [48,49]. The traps must exceed several micrometers as particles size in standard Portland concrete varies from 1 to 100 µm [50,51]. Increasing the number and size of the traps improve adherence such as acid-pickled cleaning of a hot-rolled steel that improve the adherence strength from 10^{-2} to 10^{-1}-10^{0} MPa [34]. However, which roughness parameter is most appropriate for evaluating susceptibility to mechanical anchoring remains ill-defined [52].

B. Capillary Suction

Capillary suction forms when the liquid film present along the ITZ is continuous. To obtain a continuous liquid film, a substrate surface with a high surface energy is recommended to favor the water spreading at the

interface [6]. Moreover, the hydration process must be fast as delaying the hydration induces a drop in bonding strength [53,54]. The capillary-induced bond is stronger for smooth and impermeable substrates such as steel and polymer [12,17,32]. On the contrary, water removal by absorption (e.g. on wood formworks and porous skins) reduces the water amount at the interfacial layer [55–58], weakens the capillary forces, and lowers the concrete-substrate bonding [59–61].

The chemical compounds related to the bonding of the ITZ are confined to a one molecule-thick layer at the steel surface. Therefore, the substrate surface energy, which is a measure of wettability, defines partially the extent of chemical bonding. Among the numerous characterizing methods [62,63], the sessile drop method described by the norm AFNOR EN 828 [64] enable the measurements of the physico-chemical properties of solid surfaces wetted by known liquids such as cured concrete wetted by liquid repair products [28]. The analysis is founded on the Young-Dupré equation for a perfectly flat homogeneous solid surface wetted by a liquid drop. The contact angle θ represents the interacting interfacial tensions in mechanical equilibrium (Eq. 1):

$$\sigma_{SV} = \sigma_{LS} + \sigma_{LV} \cos\theta \quad \text{(Eq. 1)}$$

, where σ_{SV} et σ_{LS} are the solid-vapor and liquid-vapor superficial tensions, respectively. The thermodynamic work of adhesion (W_a), associated to the negative of the free energy of adhesion ($-\Delta G_a$), is related to the wetting angle according to the equation of Dupré (Eq. 2):

$$W_a = \gamma_{SV} + \gamma_{LV} - \gamma_{SL} = \gamma_{LV}(1 + cos\theta) \quad \text{(Eq. 2)}$$

Adsorption of water at the steel surface is caused by primary (covalent) and secondary (dispersion, dipole and hydrogen) bond interactions between fresh concrete and metallic substrate [65]. From a thermodynamics point of view, the surface free energy γ_S can be decomposed into a polar γ_S^p and dispersive γ_S^d component [66] (Eq. 3):

$$\gamma_S = \gamma_S^d + \gamma_S^p \quad \text{(Eq. 3)}$$

To improve adhesion, the solid surface energy (γ_S) must be greater than the surface tension of wetting substances (γ_l). Since the concrete paste has a superficial surface tension of 44 mN·m^{-1} [66,67], fresh concrete strongly adhere to steel plates with surface energies between 40 and 100 mN·m^{-1} [17,68]. In opposite, the application of a layer of small surface tension substances such as release agents with active carboxyls is used on formworks to lower the substrate surface tensions and limit concrete adherence [33,69,70].

C. Electrochemical bonding

Concrete is a basic medium with unique characteristics and complex chemical and electrochemical interactions with metals, as indicated in reviews of the subject [71,72,81,73–80]. Electrochemical bonding of a concrete on metallic substrates are both electrical and chemical bonds [24,33,34]. This bonding is the result of intermolecular electromagnetic interactions progressively formed from the initial contact of the fresh semi-solid concrete until the end of its hardening stage.

Enhancing electrochemical reactions at the interface should improve concrete bonding to metallic reinforced bars. Numerous molecular interactions occur between metallic surfaces and hardening concretes: long-range Van der Walls forces (40 $kJ \cdot mol^{-1}$), short-range hydrogen bonds (50 $kJ \cdot mol^{-1}$), covalent bonds (60-700 $kJ \cdot mol^{-1}$), metallic bonds (110-260 $kJ \cdot mol^{-1}$), and ionic bonds (600-1000 $kJ \cdot mol^{-1}$). The bonding is more efficient for greater number of interfacial bonds and longer coupling molecules, e.g. the strength of London's dispersion forces increases between compounds with greater molecular weights. Hence, concrete mix, adsorption, adhesion, and kinetics of carbonation during curing are key factors for mastering electrochemical bonding formation.

The concrete hydration products react with atmospheric CO_2, humidity, and metallic hydroxides to form efflorescence (that is calcium carbonate $CaCO_3$) that grows during curing because of the high water content [8,82]. The numerous hydrated minerals present in fresh concrete, such as portlandite $Ca(OH)_2$ and hilebrandite $Ca_2[SiO_3(OH)]OH$, contain hydroxyl radicals (-OH) and have asymmetric structures. These hydrated minerals transform into the acid-basic calcium pyro-silicate referred to as afvilite $Ca_3[Si_2O_6OH]OH$ when $Ca(OH)_2$ is further being released [33]. Further hardening involve the formation in a hardened cement paste of aliphatic silicates such as the monoclinic kronotite $Ca_6Si_6O_{17}(OH)_2$ with fibrous cross-section, the fibrous tobermorite $Ca_4[Si_3O_8(OH)]OH_2$ and the hydrated ribbon silicate - girolite $Ca_4Si_6O_{15}(OH)_2$ [33].

Most metals react electrochemically in $Ca(OH)_2$-containing solutions in a similar manner than in fresh concrete [46,83–87]. Therefore it is commonly assumed that a saturated calcium hydroxide solution, with a pH of 12.6 at room temperature, may be taken as a representative electrolyte for electrochemical studies involving fresh concrete [72]. However, it remains unclear whether or not the kinetics of diffusion in saturated calcium hydroxide solutions are representative of those in concrete. Low cost and wear resistant steels are the most common materials used in formwork and reinforced bar designs [52,88]. The $K_2\ L_8\ M_{14}\ N_2$ structure of iron atoms indicates the presence of a lone pair of electrons on most external 4^{th} orbit that make the iron atoms very reactive. The electrical charging of steel surfaces by concrete friction during pouring reorganizes the ions at the interface to form a double electrical layer composed of Fe^{2+} and OH^- ions on the steel side and Ca^{2+}, Al^+ and OH^- ions on the fresh concrete side [8,10,24]. The application of release agents prior to concrete pouring generates a deflocculating action of the cement particles and stabilizes the soap-oil mecellae, isolating each ionic side from the other [16].

Cement paste contains large amount of hydroxyl radicals –OH. The high electronegativity of iron in steel (1.83) and oxygen in the radical –OH (3.44) favors the hydrogen bonding between the iron atom Fe and the radical –OH to form $Fe(OH)_2$ molecules [33] followed by the transformation of the initial impermeable oxy-hydroxide film into a porous, non-protective iron carbonate film [89]. The breakdown of this passive layer causes an increase in the substrate reactivity and corrosion rate. Hydrated FeO oxide steel surface have been associated with substrate wettability [90] and concrete adhesion [49,91,92].

Concrete bonding is stronger for thicker layers of oxide products due to the modified functional groups at the surface [49,92]. When adding weak organic acids such as oleic acid, hydroxyls react preferentially with them to form neutral non-adherent products [33]. Adhesion is also inhibited with the application of inert

surfaces on metallic substrate such as polyvinyl chloride (PVC) [8–10], polydimethylsiloxane (PDMS) [8–10], and epoxy [93]. These surfaces possess usually low wettability and small solid surface energy that enhance the water accumulation and $Ca(OH)_2$ formation in the first concrete layer according to the reaction [9]:

$$Ca(OH)_2 + CO_2 \rightarrow CaCO_3 + H_2O \quad \text{(Eq. 4)}$$

Therefore carbonation reduces by partial neutralization the alkalinity of $Ca(OH)_2$ associated to a drop of the pH from 12.4 to 11.8 [89]. This explains the increase in chemical reactions for thinner concrete bulks that is associated to easier flow of atmospheric CO_2 towards the ITZ [89]. The concrete adhesion was smaller on polyvinyl chloride (PVC) than polyoxymethylene (POM) [8,9] which may be possibly due to greater mechanical anchoring on the rougher POM material. It is noted that the epoxy-based coatings have very good corrosion resistance in alkaline concrete medium [93,94] but possess small wear resistance during concrete pouring [52].

Reinforced bars are sometimes galvanized to extend the service life of corrosion-susceptible structures [95]. Zinc is an amphoteric metal stable over a wide range of pH (6–13.2). The immersion of the galvanized rebars in alkaline solutions promotes the formation of a zinc hydroxide film (pH < 12.9) or soluble zincate ion ZnO^{2-} (pH < 12.9). However, in presence of Ca^{2+} ions, passive films of calcium hydroxizincate ($Ca(Zn(OH_3)_2.2H_2O$) are formed [96] following the sequence of reactions [3] (Eqs. 5 to 8):

$$Zn + 4OH^- \rightarrow Zn(OH)_4^{-2} + 2e^- \quad \text{(Eq. 5)}$$

$$Zn + 2OH^- \rightarrow ZnO + H_2O + 2e^- \quad \text{(Eq.6)}$$

$$ZnO + H_2O + 2OH^- \rightarrow Zn(OH)_4^{2-} \quad \text{(Eq.7)}$$

$$2Zn(OH)_4^{2-} + Ca^{2+} + 2H_2O \rightarrow Ca(Zn(OH_3)_2.2H_2O + 2OH^- \quad \text{(Eq.8)}$$

The hot-dip galvanized coating is formed of four thin layers (Figure 1) [87]: the 1st layer (outside layer) is zinc, the 2nd layer is zeta (ζ) phase, the 3rd layer is delta (δ) phase, and the 4th layer (inside layer) is steel substrate. The reactive pure zinc layer thickens with increasing hot-dip time [87].

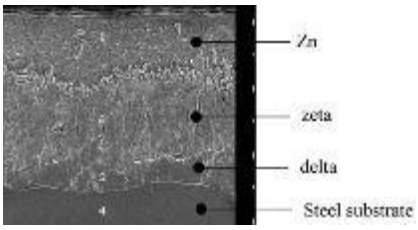

Figure 1: Scanning electron micrograph of hot-dip galvanized coating [87].

Galvanized steel is electrochemically more reactive than steel in the fresh concrete medium, leading to a 15% increase in interfacial bonding strength compared to bare steel rebar [87]. Indeed, ZnO and $Zn(OH)_2$ present at the substrate surface react with hydration compounds to initially form calcium hydroxyzincate ($CaZn_2(OH)_6{\cdot}2H_2O$) [34,54] and later $ZnSiO_4$ and $Ca_2Zn_2Si_2O_7$ after several days of curing [87]. These heavy components promote high bonding strength of concrete (up to 0.23 MPa [34,95]). However, zinc dissolution is important at pH above 13.5 [84] which produces hydrogen and modifies the cement hydration kinetics [97]. The morphology of the attack, the hydrogen evolution, and the nature of the corrosion products that are expected

are summarized in Figure 2 [3]. Chromate passivation is efficient in inhibiting the corrosion of galvanized steels [98] but is today controversial because of raised concerns on health hazards.

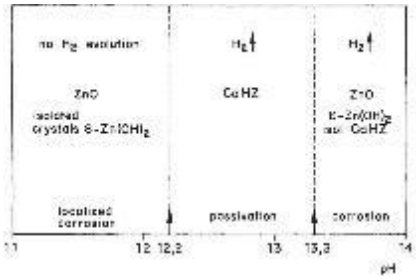

Figure 2: Behavior of galvanized rebars immersed in alkaline solutions ccontaining Ca^{2+} ions with 11-14 pH range (CaHZ = $Ca(Zn(OH)_3)_2.2H_2O$) [3]

Corrosion investigations in alkaline environments revealed that the open circuit potential (OCP) and corrosion rate were -430 mV_{SCE} and 3.0 µm/year for bare steel, and -770 mV_{SCE} and 7.8 µm/year for hot-dip galvanized steel (Figure 3) [87]. The corrosion rate was calculated using the Stern-Geary equation. The smaller corrosion potential of zinc revealed that galvanized materials are more active than bare steel in alkaline environments. The faster corrosion is related to the absence of passive film. These results in alkaline environments are in agreement with the known more reactive galvanized steel than bare steel in fresh concrete.

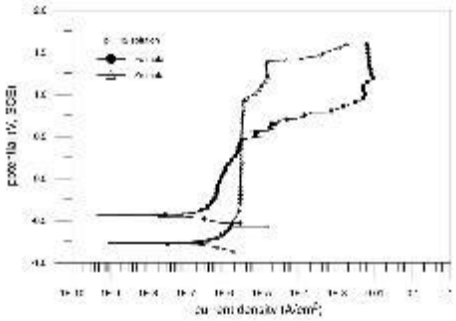

Figure 3: Potentiodynamic polarization curves in pH 12 solution [87]

Alloying zinc with passivating elements improve the corrosion resistance of galvanized coatings. Chromate [99], Ce-containing [100–105], and La-containing [106,107] conversion layers have protected efficiently galvanized steels in alkaline fresh concretes. While chromate is today avoided for its toxicity, rare-earth salts are promising alternatives. Ce-rich galvanized coatings form in alkaline environments a thick film of $Ce(OH)_3$ (outer layer) and Ce_2O_3 (inner layer) (Figure 4) that delays corrosion but only for a limited time [100]. Similarly, the formation of lanthanum oxide La_2O_3 and hydroxide $La(OH)_3$ at the La-rich galvanized surfaces delays the formation of $Ca(Zn(OH)_3)_2$ crystals when immersed in calcium-containing solutions (Figure 4) [100,108]. Aluminum doping in the galvanized coating limit the calcium hydroxizincate formation due to the preferential reaction of OH^- and $Ca(OH)_2$ with Al atoms [109,110] but the results highlight ambiguous effects on bonding strength improvement or deterioration [34,88,95].

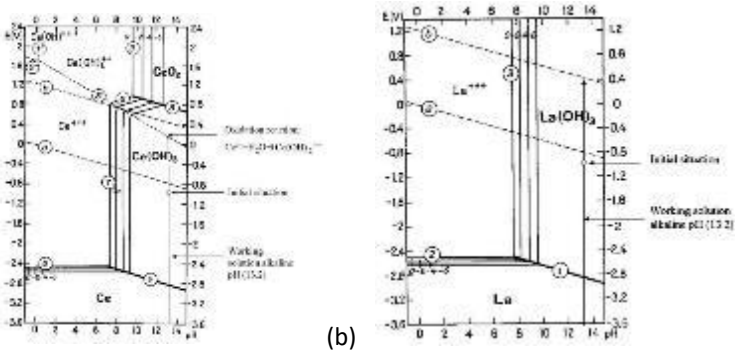

Figure 4: pH working conditions in cement superimposed to Pourbaix diagrams for (a) Ce-containing water and (b) La-containing water [100,111].

Electrochemical bonding of concrete on steel [112,113] and others metals such as Al, Zn and Pb [14] may be limited by controlling the electronic interactions with the metallic substrate polarization [114,115]. Increasing polarizing current favor the migration of water to the interface (electro-osmosis) but care must be taken to avoid the disruption of the concrete hydration by excessive water migration. Schematic principles are described in Figure 5 and polarization effect on adherence is shown in Figure 6. Maintaining steel potential at -0.4V is the condition for maximum of bonding strength. The effect of water condensation on adherence is similar to the observed drop in bonding when using concretes with high water-to-cement ratio [116].

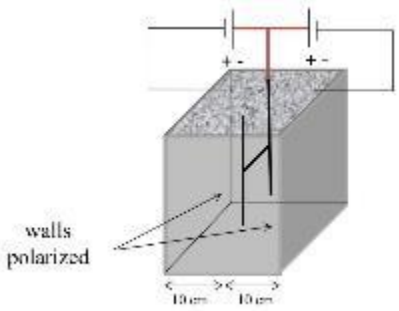

Figure 5: Experimental setup for polarization of walls in contact with concrete [112].

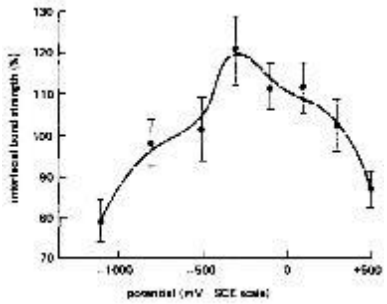

Figure 6: Effect of applied polarization of steel on bond strength with cement [113].

D. Summary

In summary, adhesion of concrete on metallic surfaces is controlled by interfacial interactions between the substrate and the curing concrete. Chemical reactivity, mechanical anchoring, and the ITZ thickness are key factors in controlling the bonding strength. The question remains whether or not one mode of adhesion is predominant. A better understanding must involve a microscopic analysis of the ITZ.

IV. Interfacial Transition Zone characterization

The bonding strength between metallic substrate and concrete has to be either minimized to avoid bonding issue during formwork removal or maximized to lengthen service life of concrete-metal composite structures. The Interfacial Transition Zone (ITZ) controls the concrete adherence. It has been characterized both chemically and mechanically.

A. ITZ Chemical Characterization

Optical and electronic microscopies have been used successfully to observe the interface between bare steel and hydrated cement paste. The ITZ size is difficult to measure but is estimated between 20 and 150 µm thick [10,54]. It exhibits porosities and a clear boundary composed of hydrated phases (Figure 7a) [27]. Elemental analyses have been performed on cross-sections of the concrete-to-steel interfaces after concrete curing to observe spatial distributions of Ca, Si, and Fe (Figure 7b) [10,27,117]. The paste fraction near the ITZ contained lot of Si and Ca-rich unhydrated cement particles while the mill scale contains many porosities [27]. X-ray diffractions demonstrated that the ITZ characteristics are influenced by the C3A/C3S ratio, and the alkaline, gypsum, and free lime contents [54].

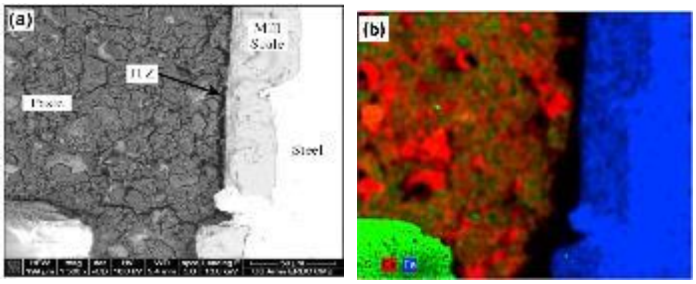

Figure 7: (a) SEM micrograph of typical microstructure present at ITZ of uncoated steel and (b) corresponding elemental mapping of Ca/Si/Fe [27].

Carbonation of the cement paste causes a drop in pH that leads to the formation of a thin, insoluble, and protective oxide layer. Back scattered electron (BSE) imaging of the first tens of micrometers of concrete along the steel surface revealed high amounts of SiO_2 [87], Ca_2SO_4 [87], $2CaOSiO_4$ [87], and $Ca(OH)_2$ [10,34]. More

$Ca(OH)_2$ molecules form when water-on-cement (w/c) ratio are high and preferentially in the ITZ rather than in the cement bulk because wall effects induce greater water amounts in the ITZ. This may lead to smaller gaps between the ITZ and the metallic substrates [35]. Calcium hydroxide $Ca(OH)_2$ contents increase during concrete hardening constantly to attain a maximum of 30% in the ITZ (Figure 8) [10]. The $Ca(OH)_2$ contents are increased when using wire-brushed, oxide-free steels because the iron atoms detached by friction from the brush onto the substrate are chemically reactive in alkaline environments. These higher amounts of calcium hydroxides in the ITZ are related to more concrete-to-steel chemical bonds, greater adherence [34], and the sudden change in mechanical properties between steel and paste [27].

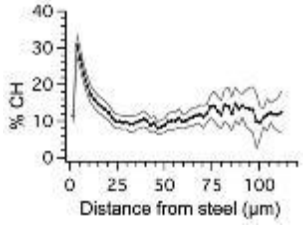

Figure 8: Microstructural gradient of calcium hydroxide (CH) at the ITZ measured by EDX [10].

Backscattered electron imaging revealed that the fractured interface between steel and concrete exhibits large $Ca(OH)_2$ crystals, porosities, and a dearth of calcium-silicate-hydrate (C–S–H) [10,27,113] (Figure 9), the whole being surrounded with a layer of cement paste [113]. As curing proceeds, the different precipitation kinetics of the various cement hydration products cause segregation and properties gradients from the concrete bulk to the ITZ-steel interface [113,118]. The compositional gradient of this segregated zone varies with sedimentation of the fresh cement paste and steel surface preparation [113].

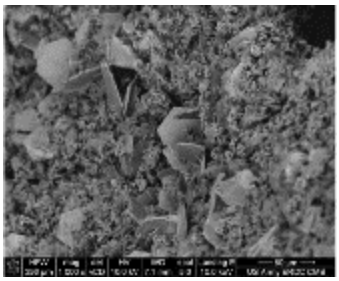

Figure 9: Typical microstructures observed on fracture surfaces at the ITZ between steel and concrete [27].

B. ITZ Mechanical Properties

1. Micro-scale properties

Concrete is composed of three superimposed layers: the cement skin (about 0.1 mm thick) against the substrate, the mortar skin (about 5 mm), and the concrete skin (about 30 mm) aside the concrete bulk [38]. The existence of these distinct layers is due to a wall effect, the sedimentation and segregation induced by gravity and compacting methods (e.g. vibrations for improving compaction), and permeation and evaporation of water

in and out of concrete. These layers generate gradients of mechanical properties across the first 5 mm of the ITZ from the metallic surface towards the concrete bulk (Figure 10) [38].

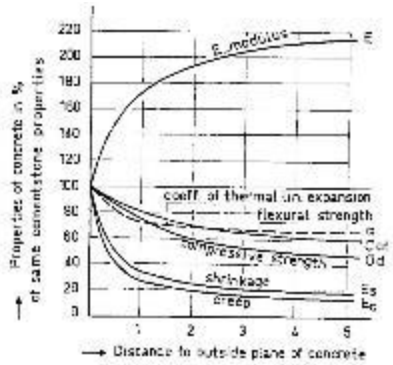

Figure 10: Mechanical properties gradients from concrete skin to 5 mm depth [38].

Depth-sensing indentations [27,37] has been performed on ITZ to provide quantitative information on Young modulus and hardness gradients at the µm-scales representative of the ITZ layers (Figure 11). Micro-indentations show variation of mechanical properties in both hardness (from 800 to 200 MPa) and elastic modulus (from 31.9 to 5.5 GPa) within the first 40 µm of the ITZ [37]. Young modulus peaks at 100 GPa were associated to unhydrated cement particles. The low mechanical properties away from the interface were associated to the $Ca(OH)_2$-rich interfacial transition zone and change with concrete formulations [27,37,54]. Nano-indentation tests with too-small normal loads did not confirm these trends because the indentation imprints became as large as the concrete porosities.

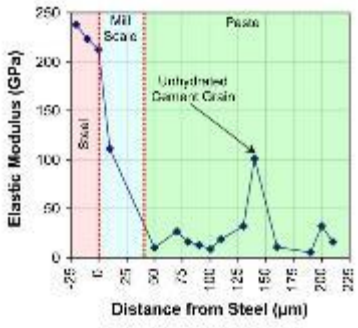

Figure 11: Evolution of elastic modulus across the ITZ between concrete and bare steel [27].

2. Macro-scale properties

The establishment of a standardized adherability test is an ongoing topic of interest for the industry as it would have the obvious advantage of enabling a reliable adherability comparison between diverse materials and concrete formulations. Even though the numerous existing laboratory tests provide a rough qualitative ranking of material adherability, the problem arises in not knowing how changes in testing procedure affect rankings and how measured data relate to real concrete fabrications. Full-scale testing has been adopted in an effort to bypass the difficulties inherent in predicting field behaviour from small-scale laboratory tests. However, due to the complexity and large dimensions of full-scale testing, laboratory-scale tests have been developed to quantify the adherability, limiting the full-scale adherability tests to a validation role for in-field applications.

There is also the inability to predict, with any certainty, whether or not bonding will indeed occur in a specific application. Nevertheless, limitations exist in providing an overview of the literature data as the broad spectrum of loading conditions, concrete formulations, and adherability test design highlight inconsistencies in the testing methodology and collected data. These discrepancies lead to a lack of understanding and disagreement on the critical factors controlling concrete adherence.

A broad variety of adherability tests has been developed over the years to investigate the steel-concrete interface, as indicated in reviews on the subject [119,120]. Testing devices include beam-end pullout specimens [33,54,87,93,94,121–130], splice specimens [121,122], beam-end test [95,98,122,128,131,132], and laboratory-scale tensile tests [68]. Conclusions must be carefully formulated as fracture modes differ between reinforced bar (shear mode) and formwork (tensile mode) adherability tests. Post-mortem fractographies revealed that the rupture involved both cohesive and adhesive failure zones [34] with a cohesive failure depending on the relative cement quality compared to the ITZ strength [24]. The concrete bulk tensile and compressive strengths are 2-to-3 MPa and 20-to-30 MPa, respectively, for a normal concrete with a w/c ratio of 0.5. Fracture should thus be adhesive if the ITZ tensile strength is lower than 2 MPa.

The single rebar pullout test is conducted following usually the ASTM C 234-91a, ASTM C234-86 or ASTM A944 specifications. A correlation has been established between interfacial toughness measured by indentation and bond strength measured by pull-out tests [116] providing a link from one scale to the other. Many theories [41,124,133–135] and numerical models [41,119,124,125,130,133,134,136] are applied to deduct the interface properties from acquired experimental curves. They usually simplified the stress state to a simple shear mode [137] even though the ITZ fracture is in reality more complicated with the involvment of many other factors such as friction [129] and important size effects [137]. Assuming a pure shear fracture, the ultimate shear stress σ_b (also referred to bonding stress or splice stress) was calculated from the maximum pullout load (P) accordingly:

$$\sigma_b = \frac{P}{\pi d l} \quad \text{(Eq. 9)}$$

, where d is the bar diameter, l is the embedded length of the bar, and πdl the interface area. The measured debonding shear stress of a steel bar from a concrete varies from 3 to 12 MPa [41,93–95,133]. The progressive increase in bonding strength during the first 28 days of concrete hardening [24,34,113,127] was attributed to the formation of an aggregate-free interfacial zone composed by segregated hydration products which attain a practically constant structure after a few days [113]. Summary of the testing data is provided in Table 1. The strength of the concrete, the roughness of the bar surface (i.e. ribbed bar), and the chemical adhesion of the concrete-steel interface are evidenced as key factors for controlling the durability of the bonds.

Low-adherence coatings are hydrophobic and thus composed of either silicone-doped polymers [8–10], fluor-plastic-doped polymers [24], fusion-bonded epoxy (FBE) chemically stable in high pH environments [138], and Bakelite-doped polymers [24]. Coatings must also possess high friction coefficients with concrete to maximize the work energy for debonding [129]. The ITZ bonding stress is promoted by the only interfacial phenomena as the expoxy-coating thickness within the range recommended by ASTM A775M/775M-93 has

negligeable effect [122]. Coating the reinforced bar with pure epoxy usually drops the bonding stress down to 2 MPa [93,94,121–124] but doping the epoxy with foreign silica sand particles provide additional friction and interlocking forces that compensate the lack of electrochemical bonding and induce an increase of bonding strength up to 10 MPa [93,94]. On the opposite, environmentally-friendly phosphate conversion, oxided surfaces, and hot-dip galvanized coatings can double the bonding strength on steel [46,49,92,94,121–123,139]. Smaller bonding strength is measured for galvanized surfaces, especially for cements with weak C3A/C3S ratio [54] because zinc delays the crystallization of calcium hydroxyzincate ($CaZn_2(OH)_6,2H_2O$) [54,96].

Table 1: Bonding strength measured between formwork and concrete

Reinforced bar		Concrete			Bonding strength		Ref
Material	**Surface finish**	**Ultimate Compressive Stress (MPa)**	**Hardening Conditions**	**Ageing Time**	**Testing Device**	**Fracture Stress (MPa)**	
Bare steel	smooth	39-67	20 °C / 100%RH	1 day	Pull-out	5-9	[140]
Bare steel	smooth	88-100	20 °C / 100%RH	28 days	Pull-out	8-10	[140]
Bare steel	rough	39-67	20 °C / 100%RH	1 day	Pull-out	13-18	[140]
Bare steel	rough	88-100	20 °C / 100%RH	28 days	Pull-out	23-27	[140]
Bare steel	smooth	15.6	-	3 days	Pull-out	6-8	[54]
Bare steel	smooth	31.3	-	28 days	Pull-out	8-14	[54]
Galvanized Steel	smooth	15.6	-	3 days	Pull-out	3-6	[54]
Galvanized Steel	smooth	31.3	-	28 days	Pull-out	4-7	[54]
Bare steel	smooth	14.6	-	3 days	Pull-out	5-6	[54]
Bare steel	smooth	29.2	-	28 days	Pull-out	8-10	[54]
Galvanized Steel	smooth	14.6	-	3 days	Pull-out	3-6	[54]
Galvanized Steel	smooth	29.2	-	28 days	Pull-out	9-13	[54]
Bare steel	smooth	-	-	28 days	Pull-out	6-8	[139]
Bare steel	smooth	-	-	7 days	Pull-out	7.8	[92]
Bare steel	smooth	-	-	28 days	Pull-out	8.2	[92]
Steel with acetone	smooth	-	-	7 days	Pull-out	6.8	[92]
Steel with acetone	smooth	-	-	28 days	Pull-out	7.5	[92]
Bare steel	smooth	21-45	-	-	Shear Test	3-30	[141]
Bare steel	smooth	44-50	-	28 days	Pull-out	5.4	[142]
Galvanized Steel	smooth	44-50	-	28 days	Pull-out	5.8	[142]
Bare steel	smooth	13-15	-	7 days	Pull-out	1-2	[33]
Acid pickled steel	smooth	40	-	-	Pull-out	0.52	[34]
Zn/Al coated steel	smooth	40	-	-	Pull-out	0.01	[34]
Bare steel	smooth	30	-	-	Pull-out	1.2-1.9	[126]
Bare steel	deformed	30	-	-	Pull-out	1.5-2.0	[126]

Most works on mechanical characterization of steel-concrete interface have been performed for reinforcing bars applications (i.e. shear strength characterization). Only few works have been devoted to formwork applications with the focus on the tensile strength measurement of the ITZ. Formowrk removal implies in fact an ITZ fracture mostly in a tensile mode. Hence, the previously described popular pullout test is efficient for reinforced bar testing but inadequate for quantification of concrete adherence on formworks. The tensile strength measured by removing full-scale formworks are consistents with laboratory-scale measurements from both a qualitative and quantitative viewpoints. Results are summarized in Table 2.

Table 2: Bonding strength measured between formwork and concrete

Formwork material	Concrete	Hardening conditions	Ageing time	Bonding strength (10^{-3} MPa)	Ref
Steel without release agents	-	17°C / 85%RH	1 days	185	[24]
Steel without release agents	-	17°C / 85%RH	3 days	489	[24]
Steel with release agent	-	17°C / 85%RH	1 days	47	[24]

Steel with release agent	-	17°C / 85%RH	3 days	142	[24]
Glass fiber reinforced plastic	-	17°C / 85%RH	1 days	21	[24]
Glass fiber reinforced plastic	-	17°C / 85%RH	3 days	26	[24]
Multi-layered compressed paper	-	17°C / 85%RH	1 days	18	[24]
Multi-layered compressed paper	-	17°C / 85%RH	3 days	18	[24]
Fluor-plastic	-	17°C / 85%RH	1 days	9	[24]
Fluor-plastic	-	17°C / 85%RH	3 days	10	[24]
Mild steel	Cement paste and mortars	-	1 day	1100-1900	[113]
			28 day	3300-5100	[113]

In conclusion, adherability quantification has been mostly performed for reinforced bars applications and little for formwork design. Unfortunately, comparison of different works is almost impracticable because of the different concrete compositions, the absence of roughness measurements on the tested substrates, and the varying testing procedures.

C. Test parameters influence

The history of pouring and curing conditions, substrate material, and concrete formulation affects concrete adherability. The amount of contraction of the concrete during curing depends on the physico-mineralogical properties and hardening conditions [24] and decreases the bonding strength if contraction is sufficient to promote interfacial micro-fractures. Interfacial bonding develops progressively during curing and drying, so the time of testing post-pouring is important. Greater bonding strength is associated to concrete in contact with rough and reactive substrates under high pressures associated to high concrete pouring heights and intense vibrations enhancing concrete penetration in the substrate interstices [24,113] (Figure 12). On the other hand, the aggregate content of the mortars does not influence the ITZ bonding strength (Figure 13) because this zone is entirely composed of cement hydration products and is free from aggregates [113]. Thus increasing the initial w/c ratio lowers the quantity of water at the interface and subsequently the amount of hydration products in the ITZ, leading to a fracture strength reduced by 10% [113].

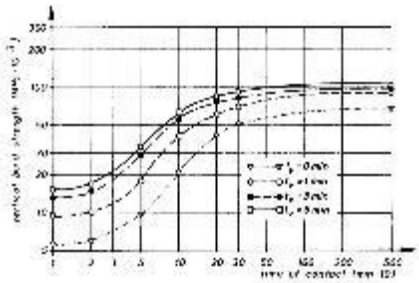

Figure 12: Influence of vibration time on bond strength between concrete and steel [24].

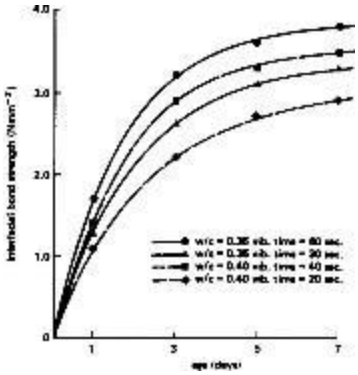

Figure 13: Effect of vibration and curing time on bond between steel and concrete [113]

V. Practical Implications

The aim of the review was to understand the underlying phenomena of concrete bonding on metallic surfaces in order to master interfacial bonding strength. Construction engineers can mitigate bonding by adjusting the concrete composition, designing properly metallic substrates, and controlling pouring and curing conditions. The following discussion demonstrates the multifaceted nature of this problem and addresses some factors that may be used by the construction engineer to control adherability.

Functional designs require understanding the dynamic interaction of concrete with metals during curing. Adhesion of concrete to metallic surfaces is proven to be a complex subject with combinations of electrochemical and mechanical factors [12,24,32,33,52]. Smooth surfaces over wide flat areas maximize capillary-induced bonding only if these surfaces possess low solid surface tensions to spread a continuous water film. Reactive surfaces lead to strong bonding because of the formation of metallic-containing hydration products. Finally, roughness has a complex role to control simultaneously mechanical anchoring, capillarity in asperities, and Wenzel versus Cassie-Baxter wetting mode. Compromises are usually required for controlling adherence. For example, epoxy coatings are used to limit corrosion of reinforced bars but simultaneously lower the bond strength of concrete to steel [98,122] leading to pros and cons for long lifespans of structures.

One particularity of formwork applications compared to reinforced bars is the wear resistance viewpoint when submitted to repetitive utilizations that lead to an evolving skin functionality pouring after pouring. In fact, polymeric skins have proven an efficient anti-adherence solution [8–10,24,93,94,98,121–124] but have weak resistance to fresh concrete-induced abrasion [52,88]. The study of concrete friction on substrates was mainly investigated using the plane/plane tribometer [16,19,21,52,88,143–150] and few rheological models [52,88,151]. The friction and wear behavior have highlighted the dependence of interfacial friction stresses of fresh concrete on a substrate with the demoulding agents [19,150,152], the aggregate contents [149], the paste volume [16] and the optional addition of superplasticizer [16,19,150]. While adding superplasticizer reduces the friction stress by deflocculating the cementious mixture [16], friction of concrete without superplasticizer involves a direct contact of granulates on the substrate surface. Substrate superfical elements are also infuencing the wear rates. Indeed, while galvanized coatings reduce the wear rates compared to bare steels [54], polymeric skins with hardnesses of the order of magnitude of 10^{-2}-10^{-1} GPa are not hard enough to resist fresh concrete-induced friction damages [52]. Wear rates are reduced as the concrete curing progressive and is thus dependent on the cement chemistry [54].

VI. Summary and perspective

The present review focused on the adherence of concrete on metallic formworks and reinforced bars. Recent developments have suggested both mechanical anchoring, capillary suction, and electrochemical bonding to play a direct role in controlling bonding strength. With advancing ideas regarding adhesion phenomena and improved testing methods, construction science is moving to a point where the overall strength of adherence may someday be predicted between a given concrete composition and a solid substrate. From a practical

standpoint, bonding strengths are difficult to measure and control, and are related to specific humidity, material, and restraining conditions (tensile versus shear). Combining experiments with segregation and mechanistic models will enable to improve the quantification of conditions needed for fracture in the ITZ to occur.

Many adherability tests have been developed to rank bonding of different concrete-substrate interfaces solely upon the fracture strength. The experiment with the application of either a shear or tensile load determines the adherence propensity and subsequently the functionality of surfaces in contact with concrete. Although useful in making rough-cut rankings, a better approach is to consider the adherability testing as an experimental means to understand the relationship between the external loading force and the local stresses in the ITZ. Nevertheless, difficulties are still encountered for the identification of the individual contribution of each component leading to the measured overall bonding strength. Further studies should be devoted in understanding the underlying mechanisms of the concrete-steel bonding interactions and the potential dominant effects of environmental conditions such as moisture, electrochemical conditions, interfacial interactions, rebar geometries, w/c ratio, curing times, and cement type.

Finally, a comment should be made on the available literature data. Reviewing the scientific publications highlighted that important experimental details were not systematically reported. This impeded the interpretation of the data and hindered the generalization of the conclusions of these specific conditions to the other experimental setups. Standardization of not only adherability test procedures, but also defining what needs to be measured will help in the long-term understanding of concrete-substrate adherability. Discrepancies in collected data are compelling arguments for developing novel design geometries of adhereability tests to enable easier access for instrumentation and facilitate the testing device as a research tool.

.

VII. References

[1] P. Coussot, C. Ancey, Rhéophysique des pâtes et des suspensions, EDP Sciences, 1999.

[2] F. de Larrard, Structure granulaires et formulation des bétons, Laboratoire central des ponts et chaussées, 1999.

[3] A.D. Wilson, J.W. Nicholson, H.J. Prosser, Surface Coatings - 2, Elsevier Applied Science, 1988.

[4] N. Holmes, K. Dunne, J. O'Donnell, Longitudinal shear resistance of composite slabs containing crumb rubber in concrete toppings, Constr. Build. Mater. 55 (2014) 365–378. https://doi.org/10.1016/j.conbuildmat.2014.01.046.

[5] M. Martin, Etude de la texture de la surface coffrée des parements verticaux en béton, Université Laval, Québec, 2007.

[6] M. Hurd, Formwork for Concrete, American Concrete Institute, 2005.

[7] CimBéton, La maîtrise esthétique des parements en béton, 2005.

[8] M. Horgnies, P. Willieme, O. Gabet, Influence of the surface properties of concrete on the adhesion of coating : Characterization of the interface by peel test and FT-IR spectroscopy, Prog. Org. Coatings. 72 (2011) 360–379. https://doi.org/10.1016/j.porgcoat.2011.05.009.

[9] M. Horgnies, Tribologie des bétons à ultra-haute performance Propriétés de surface et revêtements de protection, Tech. l'Ingénieur. TRI4600 (2012).

[10] A.T. Horne, I.G. Richardson, R.M.D. Brydson, Quantitative analysis of the microstructure of interfaces in steel reinforced concrete, Cem. Concr. Res. 37 (2007) 1613–1623. https://doi.org/10.1016/j.cemconres.2007.08.026.

[11] M.K. Hurd, High-performance plywoods for concrete forming, Concr. Constr. 202 (1997).

[12] Décollement de la pellicule de ciment, Bull. Du Cim. 37 (1969) 1–8.

[13] B. Liu, T. Yang, Y. Xie, Factors influencing bugholes on concrete surface analyzed by image processing technology, Constr. Build. Mater. 153 (2017) 897–907. https://doi.org/10.1016/j.conbuildmat.2017.07.156.

[14] B. Courtois, P. Serre, Produits de démoulage des bétons, 2007.

[15] L. Libessart, C. Djelal, P. De Caro, Influence of the type of release oil on steel formwork corrosion and facing aesthetics, Constr. Build. Mater. 68 (2014) 391–401. https://doi.org/10.1016/j.conbuildmat.2014.06.065.

[16] S. Bouharoun, Comportement tribologique des huiles de décoffrage à l'interface béton / coffrage - Influence de la formulation du béton, Université d'Artois, 2011.

[17] L. Libessart, P. De Caro, C. Djelal, I. Dubois, Correlation between adhesion energy of release agents on the formwork and demoulding performances, Constr. Build. Mater. 76 (2015) 130–139. https://doi.org/10.1016/j.conbuildmat.2014.11.061.

[18] D. Brito, R. Santos, F.A. Branco, I.S. T, R. Pais, Evaluation of the technical performance of concrete vegetable oil based release agents, Mater. Struct. 1 (2000) 262–269.

[19] C. Djelal, Y. Vanhove, P. De Caro, A. Magnin, Role of demoulding agents during self-compacting concrete casting in formwork, Mater. Struct. 35 (2002) 470–476.

[20] L. Libessart, C. Djelal, P. De Caro, I. Dubois, Influence des énergies de surfaces des huiles de démoulage sur les performances de décoffrage, in: 24èmes Rencontres Univ. Génie Civil, La Gd. Motte, 2006.

[21] C. Djelal, Y. Vanhove, D. Chambellan, P. Brisset, Influence of the application method of release agents on thickness of mould oils, Mater. Struct. 43 (2010) 687–698. https://doi.org/10.1617/s11527-009-9521-z.

[22] C. Djelal, P. de Caro, L. Libessart, I. Dubois, N. Pébère, Comprehension of demoulding mechanisms at the formwork / oil / concrete interface, Mater. Struct. 41 (2008) 571–581. https://doi.org/10.1617/s11527-

007-9268-3.

[23] J. Guichard, M. Ploton, A. Chalavon, Sheet for protecting a formwork surface, formwork installation, method of production, and method of use, WO 2016/059193 A1, 2016.

[24] A. Mazkewitsch, A. Jaworski, The adhesion between concrete and formwork, in: Adhes. between Polym. Concr., Springer, Boston, MA, 1986: pp. 67–72.

[25] M.I. Serralheiro, J. de Brito, A. Silva, Methodology for service life prediction of architectural concrete facades, Constr. Build. Mater. 133 (2017) 261–274. https://doi.org/10.1016/j.conbuildmat.2016.12.079.

[26] ACI 347-04, Guide to formwork for concrete, 2004.

[27] P.G. Allison, R.D. Moser, C.A.W. Jr, P.G. Malone, S.W. Morefield, Nanomechanical and chemical characterization of the interface between concrete , glass – ceramic bonding enamel and reinforcing steel, Constr. Build. Mater. 37 (2012) 638–644. https://doi.org/10.1016/j.conbuildmat.2012.07.066.

[28] L. Courard, Evaluation of thermodynamic properties of concrete substrates and cement slurries modified with admixtures, Mater. Struct. Constr. 34 (2002) 149–155. https://doi.org/10.1007/bf02533583.

[29] M. Pundir, M. Tirassa, M. Fernández Ruiz, A. Muttoni, G. Anciaux, Review of fundamental assumptions of the Two-Phase model for aggregate interlocking in cracked concrete using numerical methods and experimental evidence, Cem. Concr. Res. 125 (2019) 105855. https://doi.org/10.1016/j.cemconres.2019.105855.

[30] H.R. Sasse, Scientific Committeee, Adhesion between polymers and concrete: bonding·protection·repair, Springer Science and Business Media B.V., 1986. https://doi.org/10.1016/0262-5075(87)90012-1.

[31] P.H. Emmons, A.M. Vaysburd, Factors affecting the durability of concrete repair: the contractor's viewpoint, Constr. Build. Mater. 8 (1994) 5–16. https://doi.org/10.1016/0950-0618(94)90003-5.

[32] L'adhérence du béton au coffrage, Bull. Du Cim. 38–39 (1970) 1–8.

[33] J. Mlodecki, Adhesion forces of polymer modified concrete and plain concrete to steel in moulds and in reinforced concretes, in: Adhes. between Polym. Concr., Springer, Boston, MA, 1986: pp. 55–63.

[34] D.G. Montgomery, A. Samarin, Adhesion between concrete and treated or untreated flat metal surfaces, in: MRS Online Proc. Libr. Arch., 1987: pp. 263–270.

[35] F. Chen, C.Q. Li, H. Baji, B. Ma, Effect of design parameters on microstructure of steel-concrete interface in reinforced concrete, Cem. Concr. Res. 119 (2019) 1–10. https://doi.org/10.1016/j.cemconres.2019.01.005.

[36] A. Backelandt, Etude des mécanismes d'adhésion à l'interface résine/ciment en vue de la réparation des ouvrages de génie civil, INSA Lyon, 2005.

[37] W. Zhu, P.J.M. Bartos, Application of depth-sensing microindentation testing to study of interfacial transition zone in reinforced concrete, Cem. Concr. Res. 30 (2000) 1299–1304.

[38] P.C. Kreijger, The skin of concrete composition and properties, Matériaux Constr. 17 (1972) 275–283.

[39] S.J. Desouza, R.D. Hooton, J.A. Bickley, A field test for evaluating high performance concrete covercrete quality, Can. J. Civ. Eng. 25 (2011) 551–556. https://doi.org/10.1139/cjce-25-3-551.

[40] D.D. Arola, D.T. Yang, K.A. Stoffel, The apparent volume of interdigitation: A new parameter for evaluating the influence of surface topography on mechanical interlock, J. Biomed. Mater. Res. 58 (2001) 519–524. https://doi.org/10.1002/jbm.1049.

[41] H.W. Reinhardt, J. Blaauwendraad, E. Vos, Prediction of bond between steel and concrete by numerical analysis, Matériaux Constr. 17 (1984) 311–320.

[42] P.-G. de Gennes, F. Brochard-Wyart, D. Quéré, Capillarity and wetting phenomena: drops, bubbles, pearls, waves, Springer Science & Business Media, 2010.

[43] Pression du béton frais sur les coffrages, Bull. Du Cim. 26–27 (1958). https://doi.org/10.5169/seals-145523.

[44] N. Cauberg, J. Desmyter, J. Piérard, Poussée du béton autocompactant sur les coffrages, Les Dossiers Du CSTC. 3 (2006) 1–15.

[45] B.M.K. Hurd, Lateral Pressures for formwork design, Concr. Int. 29 (2007) 31–33.

[46] M.M. Jalili, S. Moradian, D. Hosseinpour, The use of inorganic conversion coatings to enhance the corrosion resistance of reinforcement and the bond strength at the rebar/concrete, Constr. Build. Mater. 23 (2009) 233–238. https://doi.org/10.1016/j.conbuildmat.2007.12.011.

[47] W. Pillard, Béton hydraulique - Mise en œuvre - Bétonnage et serrage, Tech. l'Ingénieur. C2229 V2 (2016) 1–19. http://www.techniques-ingenieur.fr/base-documentaire/42221210-les-betons-dans-la-construction/download/c2229/beton-hydraulique-mise-en-uvre-betonnage-et-serrage.html.

[48] C. Djelal, Designing and perfecting a tribometer for the study of friction of a concentrated clay-water mixture against a metallic surface, Mater. Struct. 34 (2001) 51–58.

[49] X. Fu, D.D.L. Chung, Interface between steel rebar and concrete, studied by electrochemical pull-out testing, Compos. Interfaces. 6 (1999) 81–92.

[50] C.F. Ferraris, V.A. Hackley, A.I. Avilés, Measurement of particle size distribution in portland cement powder: analysis of ASTM round robin studies, Cem. Concr. Aggregates. 26 (2004) 71–81. https://doi.org/10.1520/cca11920.

[51] C.F. Ferraris, V. a Hackley, A.I. Aviles, C.E. Buchanan, Analysis of the ASTM Round-Robin Test on Particle Size Distribution of Portland Cement : Phase II, 2002.

[52] N. Spitz, Developpement d'un procédé frugal de démoulage in situ des parois de coffrage - Etude des signatures fonctionnelles des parois de coffrage, Arts et Métiers ParisTech, 2019.

[53] A. Gmira, Etude structurale et thermodynamique d' hydrates modèles du ciment, Université d'Orléans,

2004.

[54] F. Belaïd, G. Arligule, R. François, Influence de la composition du ciment sur l'interface acier galvanisé-béton, Matériaux Tech. 87 (1999) 31–36.

[55] A.B.D. Cassie, S. Baxter, Wettability of porous surfaces, Trans. Faraday Soc. 40 (1944) 546–551. https://doi.org/10.1039/tf9444000546.

[56] J. Bico, Mécanismes d'imprégnation: Surfaces texturées, Bigouttes, Poreux, Université Paris VI, 2000.

[57] C. Chen, J. Liu, G. Cui, J. Liu, Effect of controlled permeable formwork on the improvement of concrete performances, Procedia Eng. 27 (2012) 405–411. https://doi.org/10.1016/j.proeng.2011.12.468.

[58] L. Basheer, S. V. Nanukuttan, P.A.M. Basheer, The influence of reusing "Formtex" controlled permeability formwork on strength and durability of concrete, Mater. Struct. 41 (2008) 1363–1375. https://doi.org/10.1617/s11527-007-9335-9.

[59] T. Harrison, Introducing controlled permeability formwork, Concr. Quaterly. (1990) 6–7.

[60] P.G. Malone, Use of Permeable Formwork in Placing and Curing Concrete, 1999.

[61] J. Liu, C. Miao, C. Chen, J. Liu, G. Cui, Effect and mechanism of controlled permeable formwork on concrete water adsorption, Constr. Build. Mater. 39 (2013) 129–133. https://doi.org/10.1016/j.conbuildmat.2012.05.005.

[62] I. Egry, E. Ricci, R. Novakovic, S. Ozawa, Surface tension of liquid metals and alloys-Recent developments, Adv. Colloid Interface Sci. 159 (2010) 198–212. https://doi.org/10.1016/j.cis.2010.06.009.

[63] B. Le Neindre, Tensions superficielles et interfaciales, Tech. l'Ingénieur. k475 (1993).

[64] AFNOR, NF EN 828: Adhésifs-Mouillabilité-Détermination par mesurage de l'angle de contact et de l'énergie superficielle libre de la surface, (2013).

[65] K.L. Mittal, Contact Angle, Wettability, and Adhesion - Volume 6, CRC Press, 2009. https://doi.org/10.1021/ba-1964-0043.

[66] L. Courard, F. Michel, Energies libres de surface des liquides et des solides : une approche de la comprehension des phenomenes interfaciaux, in: Compte-Rendu Des Journées Sci. Du RF 2B, 2003: pp. 1–10.

[67] L. Courard, F. Michel, M. Martin, The evaluation of the surface free energy of liquids and solids in concrete technology, Constr. Build. Mater. 25 (2011) 260–266. https://doi.org/10.1016/j.conbuildmat.2010.06.030.

[68] N. Spitz, N. Coniglio, M. El Mansori, A. Montagne, S. Mezghani, Quantitative and representative adherence assessment of coated and uncoated concrete-formwork, Surf. Coatings Technol. 352 (2018) 247–256. https://doi.org/10.1016/j.surfcoat.2018.07.098.

[69] Produits de décoffrage, Bull. Du Cim. 47 (1979). https://doi.org/10.5169/seals-145963.

[70] H. Kurt, Produits de décoffrage, Bull. Du Cim. 61 (1993).

[71] R. Myrdal, The electrochemistry and characteristics of embeddable reference electrodes for concrete, Woodhead Publishing Limited, 2007.

[72] C.L. Page, K.W.J. Treadaway, Aspects of the electrochemistry of steel in concrete, Nature. 297 (1982) 109–115.

[73] M.A. El-Reedy, Steel-reinforced concrete structures: Assessment and repair of corrosion, CRC Press, 2008. https://doi.org/10.1093/nq/CLIII.jul09.34-e.

[74] J.P. Broomfield, Corrosion of steel in concrete: understanding, investigation and repair, Taylor & Francis, 2007.

[75] K. Hermann, L. Beguine, Substances exerçant une action chimique sur le béton, Bull. Du Cim. 63 (1995).

[76] U.M. Angst, M.R. Geiker, M.C. Alonso, R. Polder, O.B. Isgor, B. Elsener, H. Wong, A. Michel, K. Hornbostel, C. Gehlen, R. François, M. Sanchez, M. Criado, H. Sørensen, C. Hansson, R. Pillai, S. Mundra, J. Gulikers, M. Raupach, J. Pacheco, A. Sagüés, The effect of the steel–concrete interface on chloride-induced corrosion initiation in concrete: a critical review by RILEM TC 262-SCI, Mater. Struct. 52 (2019) 88-. https://doi.org/10.1617/s11527-019-1387-0.

[77] H. Bohni, Corrosion in reinforced concrete structures, Woodhead Publishing Limited, 2005.

[78] A. Bentur, S. Diamond, N.S. Berke, Steel Corrosion in Concrete: fundamentals and civil engineering practice, CRC Press, 2005. https://doi.org/10.1201/9781482271898.

[79] Portland Cement Association, Corrosion of nonferrous metals in contact with fresh concrete, Mod. Concr. (1969).

[80] Le ciment et les métaux non ferreux, Bull. Du Cim. 16–17 (1948) 1–6.

[81] L. Bertolini, B. Elsener, P. Pedeferri, R. Polder, Corrosion of steel in concrete, Wiley VCH Verlag GmbH & Co. KGaA, 2004.

[82] D.E. Rogers, L.P. Aldridge, Hydrates of calcium ferrites and calcium aluminoferrites, Cem. Concr. Res. 7 (1977) 399–409. https://doi.org/10.1016/0008-8846(77)90068-0.

[83] A. Macias, C. Andrade, Corrosion of galvanized steel reinforcements in alkaline solutions, Br. Corros. J. 22 (1987) 113–118.

[84] A. Macias, C. Andrade, Corrosion of galvanized steel in dilute Ca(OH)2 solutions (pH 11.1-12.6), Br. Corros. J. 22 (1987) 162–171.

[85] B. Huet, Comportement à la corrosion des armatures dans un béton carbonaté . Influence de la chimie de la solution interstitielle et d ’une barrière de transport, Matériaux. INSA Lyon, 2005.

[86] C. Ployaert, La Corrosion des armatures des bétons armés et précontraints, 2009.

[87] A. Cheng, R. Huang, J.K. Wu, C.H. Chen, Effect of rebar coating on corrosion resistance and bond strength of reinforced concrete, Constr. Build. Mater. 19 (2005) 404–412. https://doi.org/10.1016/j.conbuildmat.2004.07.006.

[88] N. Spitz, N. Coniglio, M. El Mansori, A. Montagne, S. Mezghani, On functional signatures of bare and coated formwork skin surfaces, Constr. Build. Mater. 189 (2018) 560–567. https://doi.org/10.1016/j.conbuildmat.2018.09.042.

[89] J.K. Boah, S.K. Somuah, P. Leblanc, Electrochemical behavior of steel in saturated calcium hydroxide solution containing Cl- , SO4 2 -, and CO3 2- ions, Corrosion. 46 (1990) 153–158.

[90] M. Mantel, J.P. Wightman, Influence of the Surface Chemistry on the Wettability of Stainless Steel, Surf. Interface Anal. 21 (1994) 595–605.

[91] P. Ghods, O.B. Isgor, G. McRae, T. Miller, The effect of concrete pore solution composition on the quality of passive oxide films on black steel reinforcement, Cem. Concr. Compos. 31 (2009) 2–11. https://doi.org/10.1016/j.cemconcomp.2008.10.003.

[92] X. Fu, D.D.L. Chung, Effects of water-cement ratio, curing age, silica fume, polymer admixtures, steel surface treatments, and corrosion on bond between concrete and steel reinforcing bars, Mater. J. 95 (1998) 725–734.

[93] J. Chang, W. Yeih, The effects of particle shape on bond strength improvement of epoxy- particle coating composites, J. Mar. Sci. Technol. 9 (2001) 153–160.

[94] J.J. Chang, W. Yeih, C.L. Tsai, Enhancement of bond strength for epoxy-coated rebar using river sand, Constr. Build. Mater. 16 (2002) 465–472. https://doi.org/10.1016/S0950-0618(02)00101-0.

[95] B.F. Tutikian, T. Hilgert, J.J. Howland, Adherence comparison of concrete with unprotected steel and hot galvanized steel, Ibracon Struct. Mater. J. 7 (2014) 313–320.

[96] F. Liebau, A. Amel-Zadeh, The Crystal Structure of Ca[Zn,(OH),] - 2 H,O - a Retarder in the Setting of Portland Cement, Krist. Und Tech. 7 (1972) 221–227.

[97] G. Arliguie, J. Grandet, Etude par calorimetrie de l'hydratation du ciment portland en presence de zinc, Cem. Concr. Res. 15 (1985) 825–832.

[98] O.A. Kayyali, S.R. Yeomans, Bond and slip of coated reinforcement in concrete, Constr. Build. Mater. 9 (1995) 219–226. https://doi.org/10.1016/0950-0618(95)00024-A.

[99] M.F. Montemor, A.M. Simões, M.G.S. Ferreira, Composition and behaviour of cerium films on galvanised steel, Prog. Org. Coatings. 43 (2001) 274–281.

[100] M. Sánchez, M.C. Alonso, P. Cecílio, M.F. Montemor, C. Andrade, Electrochemical and analytical assessment of galvanized steel reinforcement pre-treated with Ce and la salts under alkaline media, Cem. Concr. Compos. 28 (2006) 256–266. https://doi.org/10.1016/j.cemconcomp.2006.01.004.

[101] M.F. Montemor, A.M. Simões, M.G.S. Ferreira, Composition and corrosion behaviour of galvanised steel treated with rare-earth salts : the effect of the cation, Prog. Org. Coatings. 44 (2002) 111–120.

[102] W. Trabelsi, P. Cecilio, M.G.S. Ferreira, M.F. Montemor, Electrochemical assessment of the self-healing properties of Ce-doped silane solutions for the pre-treatment of galvanised steel substrates, Prog. Org. Coatings. 54 (2005) 276–284. https://doi.org/10.1016/j.porgcoat.2005.07.006.

[103] K. Aramaki, Self-healing mechanism of an organosiloxane polymer film containing sodium silicate and cerium (III) nitrate for corrosion of scratched zinc surface in 0 . 5 M NaCl, Corros. Sci. 44 (2002) 1621–1632.

[104] K. Aramaki, Preparation of chromate-free , self-healing polymer films containing sodium silicate on zinc pretreated in a cerium (III) nitrate solution for preventing zinc corrosion at scratches in 0 . 5 M NaCl, Corros. Sci. 44 (2002) 1375–1389.

[105] K. Aramaki, Treatment of zinc surface with cerium (III) nitrate to prevent zinc corrosion in aerated 0.5 M NaCl, Corros. Sci. 43 (2001) 2201–2215.

[106] A.L. Rudd, C.B. Breslin, F. Mansfeld, The corrosion protection a orded by rare earth conversion coatings applied to magnesium, Corros. Sci. 42 (2000) 275–288.

[107] S. Bernal, F.J. Botana, J.J. Calvino, M. Marcos, J.A. Pérez-Omil, H. Vidal, Lanthanide salts as alternative corrosion inhibitors, J. Alloys Compd. 225 (1995) 638–641. https://doi.org/10.1016/0925-8388(94)07135-7.

[108] B.R.W. Hinton, L. Wilson, The corrosion inhibition of zinc with cerous chloride, Corros. Sci. 29 (1989). https://doi.org/10.1016/0010-938X(89)90087-5.

[109] La corrosion de l'aluminium par le mortier de ciment, Bull. Du Cim. 34–35 (1966) 1–6.

[110] CSTB, CEBTP, VERITAS, CETEN_APAVE, SOCOTEC, NORISKO_Construction, SNFA, QUALICONSULT, Comportement de l'aluminium et ses alliages utilisés dans le bâtiment en contact avec le plâtre ou le ciment ainsi que d'autres matériaux, 2008.

[111] A. Pourbaix, Atlas of electrochemical equilibria in aqueous solutions, National Association of Corrosion Engineers, Houston, TX, 1974.

[112] N. Goudjil, Y. Vanhove, C. Djelal, H. Kada, Development of a New Demoulding Process Based on Concrete Polarization, 15th Int. Conf. Exp. Mech. (2012) 1–16.

[113] C.L. Page, M.N. Al Khalaf, A.G.B. Ritchie, Steel/mortar interfaces: mechanical characteristics and electrocapillarity, Cem. Concr. Res. 8 (1978) 481–490. https://doi.org/10.1016/0008-8846(78)90028-5.

[114] N. Goudjil, Développement d'un nouveau procédé de décoffrage basé sur la polarisation du béton – Etude de l'aspect des parements en béton, Université d'Artois, 2011.

[115] P.M. Chess, Cathodic protection of steel in concrete, 2005.

https://doi.org/10.1017/CBO9781107415324.004.

[116] S. Grairia, Y. Chrait, A. Montagne, D. Chicot, A. Iost, Interfacial Indentation Test for the Study of Reinforcement bar / concrete matrix Adhesion in High Performance Self Compacting Concretes, JMESCN. 9 (2018) 189–200.

[117] T.D. Nguyen, Etude de la zone d ’ interphase ” granulats calcaires poreux-pâte de ciment": influence des propriétés physico-mécaniques des granulats. Conséquences sur les propriétés mécaniques du mortier, Ecole Nationale Supérieure des Mines de Saint-Etienne, 2013.

[118] T.A. Soylev, R. François, Quality of steel-concrete interface and corrosion of reinforcing steel, Cem. Concr. Res. 33 (2003) 1407–1415. https://doi.org/10.1016/S0008-8846(03)00087-5.

[119] T.S. Phan, Modélisation numérique de l ’ interface acier-béton : Application au comportement des structures en béton renforcées par des aciers plats crantés, Université Paris Est, 2012.

[120] N.D. Ramirez, Etude de la liaison acier-béton : de la modélisation du phénomène à la formulation d’un élément fini enrichi “béton armé,” Ecole normale supérieure de Cachan, 2005.

[121] C.J. Hester, S. Salamizavaregh, D. Darwin, S.L. Mccabe, Bond of epoxy-coated eeinforcement : splices, ACI Struct. J. 90 (1993) 89–102.

[122] O.C. Choi, H. Hadje-Ghaffari, D. Darwin, S.L. McCabe, Bond of epoxy-coated reinforcement: bar parameters, ACI Struct. J. 88 (1991) 207–217.

[123] M.M. El-Hawary, Evaluation of bond strength of epoxy-coated bars in concrete exposed to marine environment, Constr. Build. Mater. 13 (1999) 357–362. https://doi.org/10.1016/S0950-0618(99)00042-2.

[124] W. Yeih, R. Huang, J.J. Chang, C.C. Yang, Pullout test for determining interface properties between rebar and concrete, Adv. Cem. Based Mater. 5 (1997) 57–65. https://doi.org/10.1016/S1065-7355(96)00004-1.

[125] B. Luccioni, G. Ruano, F. Isla, R. Zerbino, G. Giaccio, A simple approach to model SFRC, Constr. Build. Mater. 37 (2012) 111–124. https://doi.org/10.1016/j.conbuildmat.2012.07.027.

[126] K.M. Anwar Hossain, Bond characteristics of plain and deformed bars in lightweight pumice concrete, Constr. Build. Mater. 22 (2008) 1491–1499. https://doi.org/10.1016/j.conbuildmat.2007.03.025.

[127] J.F. Berthet, I. Yurtdas, Y. Delmas, A. Li, Evaluation of the adhesion resistance between steel and concrete by push out test, Int. J. Adhes. Adhes. 31 (2011) 75–83. https://doi.org/10.1016/j.ijadhadh.2010.11.004.

[128] L.A. Lutz, P. Gergely, Mechanics of bond and slip of deformed bars in concrete, ACI J. (1967) 711–721.

[129] M. Raous, M.A. Karray, Model coupling friction and adhesion for steel-concrete interfaces, Int. J. Comput. Appl. Technol. 34 (2009) 42–51. https://doi.org/10.1504/IJCAT.2009.022701.

[130] K. El Cheikh, Étude de l’interface milieu granulaire – paroi rugueuse par approches expérimentale et

numérique – Application aux bétons, Université d'Artois et Ecole nationale supérieure des Mines Douai, 2015.

[131] G.R. Antunes, Â.B. Masuero, Flexural tensile strength in mortar coating reinforced with different types of metal mesh: A statistical comparison, Constr. Build. Mater. 121 (2016) 559–568. https://doi.org/10.1016/j.conbuildmat.2016.06.033.

[132] A. Bideci, H. Öztürk, Ö.S. Bideci, M. Emiroğlu, Fracture energy and mechanical characteristics of self-compacting concretes including waste bladder tyre, Constr. Build. Mater. 149 (2017) 669–678. https://doi.org/10.1016/j.conbuildmat.2017.05.191.

[133] H. Stang, Z. Li, S.P. Shah, Pullout problem: stress versus fracture mechanical approach, J. Eng. Mech. 116 (1990) 2136–2150.

[134] A.S. Ezeldin, P.N. Balaguru, Characterization of bond between fiber concrete and reinforcing bars using nonlinear finite element analysis, Comput. Struct. 37 (1990) 569–584. https://doi.org/10.1016/0045-7949(90)90046-5.

[135] L' adhérence béton - acier, Tech. l'Ingénieur. TBA1125 (2006) 0–19.

[136] D.F. Laefer, A. Erkal, Selection, production, and testing of scaled reinforced concrete models and their components, Constr. Build. Mater. 126 (2016) 398–409. https://doi.org/10.1016/j.conbuildmat.2016.08.129.

[137] Z.P. Bazant, S. Sener, Size effect in pullout tests, ACI Mater. J. Sept-Nov (1988) 347–351.

[138] A.B. Darwin, J.D. Scantlebury, Retarding of corrosion processes on reinforcement bar in concrete with an FBE coating, Cem. Concr. Compos. 24 (2002) 73–78. https://doi.org/10.1016/S0958-9465(01)00028-2.

[139] X. Fu, D.D.L. Chung, Linear correlation of bond strength and contact electrical resistivity between steel rebar and concrete, Cem. Concr. Res. 25 (1995) 1397–1402. https://doi.org/10.1016/0008-8846(95)00133-W.

[140] A. Hamouine, M. Lorrain, Etude de la résistance à l'arrachement de barres enrobées dans du béton de hautes performances, Mater. Struct. 28 (1995) 569–574. https://doi.org/10.1007/BF02473188.

[141] W. Kurz, C. Kessler, P.L. Geiss, S. Turcinskas, Evaluation of adhesive bonding between steel and concrete, in: Compos. Constr. Steel Concr. VI, 2011: pp. 669–679.

[142] L. Maldonado, O. Quiroz-Zavala, L. Díaz-Ballote, Bond between galvanized steel and concrete prepared with limestone aggregates, Anti-Corrosion Methods Mater. 57 (2010) 305–313. https://doi.org/10.1108/00035591011087163.

[143] B. Bhushan, J.N. Israelachvili, U. Landman, Nanotribology: Friction, wear and lubrication at the atomic scale, Nature. 374 (1995) 607–616. https://doi.org/10.1038/374607a0.

[144] P.F.G. Banfill, The rheology of fresh mortar, Mag. Concr. Res. 43 (1991) 13–21.

https://doi.org/10.1680/macr.1991.43.154.13.

[145] S. Bouharoun, Y. Vanhove, C. Djelal, P. De Caro, I. Dubois, Interactions between superplasticizer and release agents at the concrete / formwork interface, Mater. Sci. Appl. 3 (2012) 384–389.

[146] Y. Vanhove, C. Djelal, T. Chartier, Ultrasonic wave reflection approach to evaluation of fresh concrete friction, J. Adv. Concr. Technol. 6 (2008) 253–261.

[147] C. Djelal, Y. Vanhove, A. Magnin, Tribological behaviour of self compacting concrete, Cem. Concr. Res. 34 (2004) 821–828. https://doi.org/10.1016/j.cemconres.2003.09.013.

[148] S. Bouharoun, P. De Caro, I. Dubois, C. Djelal, Y. Vanhove, Effect of a superplasticizer on the properties of the concrete/oil/formwork interface, Constr. Build. Mater. 47 (2013) 1137–1144. https://doi.org/10.1016/j.conbuildmat.2013.05.029.

[149] Y. Vanhove, C. Djelal, A. Magnin, A device for studying fresh concrete friction, Cem. Concr. Aggregates. 26 (2004) 35–41. https://doi.org/10.1520/cca11897.

[150] C. Djelal, Y. Vanhove, L. Libessart, Analysis of friction and lubrication conditions of concrete/formwork interfaces, Int. J. Civ. Eng. Technol. 7 (2016) 18–30.

[151] C. Ferraris, F. Larrard, N. Martys, Fresh concrete rheology: recent developments, in: Mater. Sci. Concr. VI, Amer. Cer. Soc. Ed. S. Mindess, J. Skalny, 2001: pp. 215–241.

[152] L. Libessart, Influence de la composition des agents de démoulage à l'interface coffrage / béton - Impact sur l'esthétique des parements en béton, Université d'Artois, 2006.